

# Level spectroscopy of the square-lattice three-state Potts model with a ferromagnetic next-nearest-neighbor coupling

Hiroshi Otsuka, Koutaro Mori, and Yutaka Okabe

*Department of Physics, Tokyo Metropolitan University, Tokyo 192-0397 Japan*

Kiyohide Nomura<sup>1</sup>

<sup>1</sup>*Department of Physics, Kyushu University, Fukuoka 812-8581 Japan*

(Received 30 December 2004; revised manuscript received 22 June 2005; published 5 October 2005)

We study the square-lattice three-state Potts model with the ferromagnetic next-nearest-neighbor coupling at finite temperature. Using the level-spectroscopy method, we numerically analyze the excitation spectrum of the transfer matrices and precisely determine the global phase diagram. Then we find that, contrary to a previous result based on the finite-size scaling, the massless region continues up to the decoupling point with  $\mathbf{Z}_3 \times \mathbf{Z}_3$  criticality in the antiferromagnetic region. We also check the universal relations among excitation levels to provide the reliability of our result.

DOI: [10.1103/PhysRevE.72.046103](https://doi.org/10.1103/PhysRevE.72.046103)

PACS number(s): 05.50.+q, 05.70.Jk, 64.60.Fr

The concept of the Gaussian universality class provides a paradigm for the unified descriptions and understanding of the low-energy and long-distance properties of one-dimensional (1D) quantum and two-dimensional (2D) classical systems. Its representation is given by the free-boson fixed point model, and its criticality by the conformal field theory (CFT) with the central charge  $c=1$ . The antiferromagnetic three-state Potts (AF3SP) model on the square lattice is one of those to exhibit the Gaussian criticality at zero temperature [1,2]. While the ground-state [1–6] and finite-temperature properties [7] were fully clarified, there still exists considerable interest in its related extended-type models [3,8,9]. For instance, in [9], the emergence of the  $\mathbf{Z}_2$  and  $\mathbf{Z}_3$  criticalities were studied by introducing the AF3SP model with a staggered polarization field.

In this paper we treat another model with a rather straightforward extension, i.e., the three-state Potts model with ferromagnetic next-nearest-neighbor coupling defined on the square lattice  $\Lambda$ , whose reduced Hamiltonian  $\mathcal{H}(K_1, K_2) = H/k_B T$  is given as

$$\mathcal{H}(K_1, K_2) = K_1 \sum_{\langle j,k \rangle} \delta_{\sigma_j, \sigma_k} - |K_2| \sum_{[j,k]} \delta_{\sigma_j, \sigma_k}. \quad (1)$$

The first and the second sums run over all nearest-neighbor and next-nearest-neighbor pairs, respectively, and the ternary variables  $\sigma_j$  take the values 0,1,2 ( $j \in \Lambda$ ). For the AF case ( $K_1 > 0$ ), this model is thought to be in the same universality class as the ferromagnetic six-state clock (F6SC) model [10]. Theoretical investigations including numerical ones have been performed to clarify the global phase diagram [3,11,12]. However, its precise estimation is not available. This is mainly because two types of Berezinskii-Kosterlitz-Thouless (BKT) transitions take part in the phase diagram, and the numerical methods used so far were insufficient to treat the BKT transitions. For instance, the phenomenological renormalization-group (PRG) method has been frequently used for the determination of second-order transition points. However, as pointed out by several authors, it fails to esti-

mate the BKT points [13]. Therefore, a new strategy should be employed. In investigations of 1D quantum systems, the level-spectroscopy method which takes logarithmic corrections into account has been used for precise estimates of the BKT points, and its possible application to the 2D classical system was also discussed [14]. Therefore, we shall reconsider this long-standing model (1) with a different methodological strategy in order to clarify the global phase diagram. While the detail is given in the following, the data obtained here agree with the exact results available in some limits of model parameters, and show that the phase diagram is constructed by the crossover of the criticality from the decoupling point  $(K_1, K_2) = (0, \ln(1 + \sqrt{3}))$  with  $\mathbf{Z}_3 \times \mathbf{Z}_3$  criticality ( $c = \frac{8}{5}$ ), which is in contrast to the previous result based on the naive finite-size-scaling method [3]. As a result, the precise determination of the phase diagram around the point turns out to be crucial to understand this model, whereas the Coulomb-gas picture provides a quantitative description only around the  $K_1 = +\infty$  line.

Here we shall briefly refer to some relevant researches. First, the ground state of the AF3SP model ( $K_1 = +\infty, K_2 = 0$ ), which is equivalent to the ice-point six-vertex model and is thus critical [2], becomes off-critical at finite temperature [15]. It was pointed out that there are two types of excitations controlled by the thermal scaling field  $u = e^{-K_1}$ , i.e., the relevant and the marginal ones, and that both of these are necessary to explain the exotic corrections to scaling observed in the Monte Carlo data [7]. The energy operator  $\epsilon_j = \sum_{\langle j,k \rangle} \delta_{\sigma_j, \sigma_k}$  (the scaling dimension  $x_\epsilon = \frac{3}{2}$ ) is the relevant excitation and brings about the correlation length  $\xi \propto u^{-1/(2-x_\epsilon)}$  in its leading form. According to Delfino, the dual sine-Gordon Lagrangian density in term of the bosonic field and its dual field  $\phi, \theta \in [0, 2\pi/\sqrt{2}]$  can describe this transition:

$$\mathcal{L} = \frac{1}{2\pi K} (\nabla \phi)^2 + \frac{1}{2\pi \alpha^2} (y \cos 6\sqrt{2}\phi + \bar{y} \cos \sqrt{2}\theta), \quad (2)$$

where  $y$  and  $\bar{y} \propto u$  are the coupling constants and  $\alpha$  is a short-distance cutoff [5,7]. Since the Gaussian coupling  $K$  is  $\frac{1}{3}$  for

the AF3SP model at zero temperature, and thus the second term, the  $\mathbf{Z}_6$  symmetry-breaking field, with the scaling dimension 6 is highly irrelevant to this transition, we can drop it for the discussions of the AF3SP model. However, it can become relevant for nonzero  $K_2 > 0$  (see below).

Next, let us consider the case with  $u=0$  ( $K_1 = +\infty$ ), where Eq. (1) is equivalent to the exactly solved  $F$  model [16]. Define  $v=e^{K_2}$ ; then the  $v$  dependence of the Gaussian coupling is given as  $1/9K=1-(1/\pi)\cos^{-1}(v^2/2-1)$  [17]. Thus the point  $v_2=2$  (i.e.,  $K=\frac{1}{9}$ ) separates the massless ( $v \leq v_2$ ) and the massive ( $v > v_2$ ) regions with sixfold degeneracy, and the latter is stabilized by the relevant term  $y \cos 6\sqrt{2}\phi$ . Further, the nonlinear terms in Eq. (2) are both irrelevant in the region  $v_1 \leq v \leq v_2$  with  $v_1 = \sqrt{2+2\cos(5\pi/9)} \approx 1.2856$  ( $K=\frac{1}{4}$ ), so the critical phase spreads at least for small  $u$  and connects to the region in the limit  $u \rightarrow 0$  [3]. This argument is consistent with the so-called cell-spin analysis [18]: Park showed that Eq. (1) with  $K_2=K_1/2$  is approximately reduced to the F6SC model in terms of the cell spins representing the unit cells of the sixfold ground states. Therefore, as a member of the F6SC universality class [19], the present model (1) is also expected to possess two BKT points  $v_1(u)$  and  $v_2(u)$ , which is described by the dual sine-Gordon field theory Eq. (2).

We shall first consider the system around  $v_1(u)$  where  $\cos 6\sqrt{2}\phi$  is irrelevant, and thus it is described by

$$\mathcal{L}_1 = \frac{1}{2\pi K}(\nabla\phi)^2 + \frac{\bar{y}}{2\pi\alpha^2}\cos\sqrt{2}\theta, \quad K \approx \frac{1}{4}. \quad (3)$$

One of the authors (K.N.) investigated the properties of marginal operators on the BKT line: Especially, in this case,  $(1/K)(\nabla\phi)^2$  and  $\sqrt{2}\cos\sqrt{2}\theta$  (the bosonized expression of  $\epsilon_j$ ) hybridize along the renormalization-group flow and result in two orthogonalized operators, i.e., the “ $\mathcal{M}$ -like” and the “cos-like” operators [14]. Writing the former and the latter as  $\bar{O}_0$  and  $\bar{O}_1$ , and defining the system on  $\Lambda$  with  $M(\rightarrow\infty)$  rows of  $L$  sites wrapped on a cylinder, near the multicritical point, their renormalized scaling dimensions are given as  $\bar{x}_0(l) \approx 2 - y_0(1 + \frac{4}{3}t)$  and  $\bar{x}_1(l) \approx 2 + y_0(2 + \frac{4}{3}t)$ , where  $l = \ln L$ ,  $(y_0, y_1) = (1/2K - 2, \bar{y})$ , and the small deviation from the BKT point  $t = y_1/y_0 - 1$ . Since these operators are parts of  $\mathcal{L}_1$ , the corresponding excitations possess the same symmetry with the ground state (see below). Another important operator is a relevant one:  $O_2 = \sqrt{2}\sin 3\sqrt{2}\phi$  whose dimension is expressed as  $x_2(l) \approx \frac{9}{16}(2 - y_0)$  in the same region. Consequently, the level-crossing condition  $\bar{x}_0(l) = \frac{16}{9}x_2(l)$  offers a finite-size estimate of the BKT point  $v_1(u, L)$  [14].

Next we consider a region near  $v_2(u)$  where  $\cos\sqrt{2}\theta$  is irrelevant. The effective Lagrangian is then given as

$$\mathcal{L}_2 = \frac{1}{2\pi K}(\nabla\phi)^2 + \frac{y}{2\pi\alpha^2}\cos 6\sqrt{2}\phi, \quad K \approx \frac{1}{9}. \quad (4)$$

In this case, the marginal operators  $(1/K)(\nabla\phi)^2$  and  $\sqrt{2}\cos 6\sqrt{2}\phi$  also hybridize and result in the  $\mathcal{M}$ -like and cos-like operators,  $O_0$  and  $O_1$ . Then, their scaling dimensions near the transition point are  $x_0(l) \approx 2 - y_0(1 + \frac{4}{3}t)$  and  $x_1(l)$

$\approx 2 + y_0(2 + \frac{4}{3}t)$ . Here,  $(y_0, y_1) = (18K - 2, y)$  have been redefined. The operator  $O_2$  has the dimension  $x_2(l) \approx \frac{1}{4}[2 - y_0(1 + 2t)]$ . Thus, the level-crossing condition for  $v_2(u, L)$  can be given by  $x_0(l) = 4x_2(l)$ . Although there may exist some other level-crossing conditions for the determination of the BKT points, the levels focused on here and used in the following are relatively easy to access by numerical calculations [20].

Now, let us consider the system on  $\Lambda$  with  $M(\rightarrow\infty)$  rows of  $L$  (an even number) sites, where  $j \in \Lambda$  is specified by  $l \in [1, L]$  and  $m \in [1, \infty]$ . For this system, we can define the transfer matrix  $\mathbf{T}(L)$  connecting  $(\sigma_{1,m}, \dots, \sigma_{L,m})$  to  $(\sigma_{1,m+1}, \dots, \sigma_{L,m+1})$ , and denote its eigenvalues as  $\{\lambda_n(L)\}$  or their logarithms as  $\{E_n(L) = -\ln|\lambda_n(L)|\}$  ( $n$  specifies a level). Then CFT provides direct expressions for  $c$  and  $x_n$  (the scaling dimensions) of critical systems as  $E_g(L) \approx Lf - \pi v c / 6L + b/L^3$  and  $\Delta E_n(L) \approx (2\pi v / L)x_n$ , where  $E_g$  is the smallest one corresponding to the ground state and  $\Delta E_n(L) = E_n(L) - E_g(L)$  is an excitation gap [21,22].  $1/v, f$ , and  $b$  are the geometric factor ( $v=1$ ), the free energy per site, and a non-universal constant, respectively. While we can calculate the renormalized scaling dimension  $x_n(l)$  from the excitation gap as  $\Delta E_n(L)/(2\pi v/L)$ , the symmetry properties are important for the specification of relevant excitations [9]. In addition to the translation  $\mathcal{T}$  and the space inversion  $\mathcal{P}$ , the  $\mathbf{S}_3$  symmetry associated with the global permutations of the ternary variables is also possessed by the present model (1). By defining the clock variable as  $s_j = e^{i2\pi\sigma_j^3}$ , the two generators of the  $\mathbf{S}_3$  group are expressed as the cyclic permutation  $\mathcal{S}: s_j \mapsto e^{i2\pi/3}s_j$  for the  $\mathbf{Z}_3$  symmetry and the charge conjugation  $\mathcal{C}: s_j \mapsto s_j^*$  for the charge conjugation symmetry ( $\mathbf{C}$ ). These operations are then related to the changes of the phase variable as  $\mathcal{S}: \sqrt{2}\phi \mapsto \sqrt{2}\phi + 2\pi/3$  and  $\mathcal{C}: \sqrt{2}\phi \mapsto -\sqrt{2}\phi$  [5]. Apparently the marginal operators defined above are  $\mathbf{S}_3$  invariant, and thus the corresponding excitation levels  $\Delta E_n(L)$  should be found in the subspace specified by this symmetry property. On the other hand, the relevant operator  $O_2$  is  $\mathbf{Z}_3$  invariant, but is odd for the charge conjugation. Further, since the sublattice symmetry property is determined by the  $\mathbf{Z}_3$  charge [5],  $O_2$  is odd for this symmetry operation. Therefore, we calculate the excitation levels according to the indices for these symmetry operations.

The exact diagonalization calculations of  $\mathbf{T}(L)$  are carried out for systems with  $L=8-16$ . In Figs. 1(a) and 1(b), we plot examples of the  $K_2$  dependencies of the scaled gaps  $x_n = \Delta E_n(K_1, K_2, L)/(2\pi v/L)$  (or values multiplied by constants) at  $K_1=1$ . Then, we find the points [i.e., the finite-size estimates  $v_{1,2}(u, L)$ ] at which one of the above conditions is satisfied. Here, it is worthy of note that, in addition to the logarithmic correction, there is another type of correction between a lattice system and a continuous model which stems from the  $x=4$  irrelevant operator  $L_{-2}\bar{L}_{-2}\mathbf{1}$  in terms of CFT [23]. Therefore, we shall extrapolate them to the thermodynamic limit according to the least-squares fitting of the polynomials in  $1/L^2$ . In Table I, we give  $v_{1,2}(u, L)$  at  $K_1=64$  (i.e., a case almost equivalent to the  $F$  model) in order to compare our data with the exact limiting values  $v_{1,2}$ . While considerable size dependencies are visible in the estimates, we can check that the extrapolated data do not deviate more than 0.7% from the exact ones.

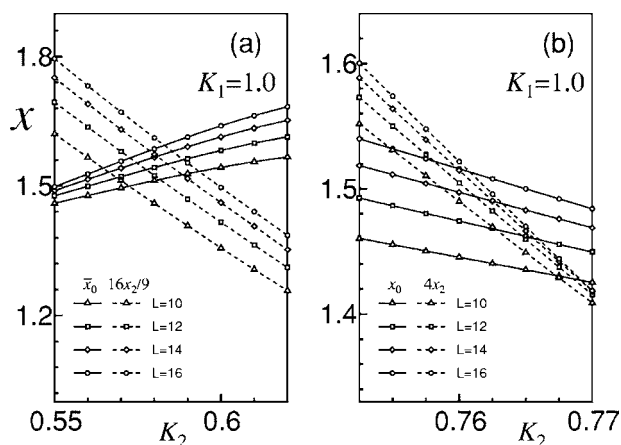


FIG. 1. Examples of the  $K_2$  dependence of scaling dimensions  $\Delta E_n(K_1, K_2, L)/(2\pi v/L)$  at  $K_1=1$ . (a) [(b)] shows  $\bar{x}_0$  and  $16x_2/9$  ( $x_0$  and  $4x_2$ ). The correspondences between marks and system sizes are given in these panels. The crossing points give finite-size estimates  $v_{1,2}(u, L)$ .

In Fig. 2, we give the phase diagram of our model (1) in the space  $(u, v) = (e^{-K_1}, e^{K_2})$ . The open diamonds (squares) with a curve exhibit the phase boundary  $v_1(u)$  [ $v_2(u)$ ], which separates the critical region from the disordered phase [from the ordered phase “Ordered (I)” with sixfold degeneracy]. The filled diamond and the square on the  $v$  axis show  $(0, v_1)$  and  $(0, v_2)$ , respectively. The filled circle at  $(u, v) = (1, 1 + \sqrt{3})$  denotes the decoupling point with  $\mathbf{Z}_3 \times \mathbf{Z}_3$  criticality [24]. To complete the phase diagram, we also calculate the second-order phase transition point  $v_3(u)$  with the ferromagnetic three-state Potts (F3SP) criticality in the ferromagnetic region  $u > 1$  (i.e., triangles) by employing the PRG method [3]. The ordered phase “Ordered (II)” has threefold degeneracy, and the thick dotted line shows the first-order phase transition boundary. From this figure we can find the following. While the cusplike behavior of the phase diagram is observed around the decoupling point [25], two BKT lines  $v_{1,2}(u)$  do not merge into a single curve contrary to the observation in the previous work based on the PRG calculation [3]. Therefore, we conclude that the massless critical region continues up to the decoupling point and that neither a critical end point nor a first-order transition line exists in the antiferromagnetic region  $u < 1$ . Further, contrary to the previous calculation, the  $u$  dependence of  $v_2(u)$  is monotonic and does not show a minimum around  $u \approx 0.3$ . As a result, the phase diagram obtained by the level-spectroscopy method is considerably different from the previous one, and shows that the Gaussian critical region is stabilized in a wider area of the parameter space.

TABLE I. The finite-size estimates of the BKT points for systems close to the  $F$  model [ $v_{1,2}(0, L)$ ]. Extrapolations to  $L \rightarrow \infty$  are performed according to the least-squares fitting of the polynomials in  $1/L^2$ .

$L$	8	10	12	14	16	$\infty$
$v_1(0, L)$	1.31465	1.30449	1.29871	1.29517	1.29287	1.285
$v_2(0, L)$	2.02507	2.02626	2.02541	2.02404	2.02262	2.013

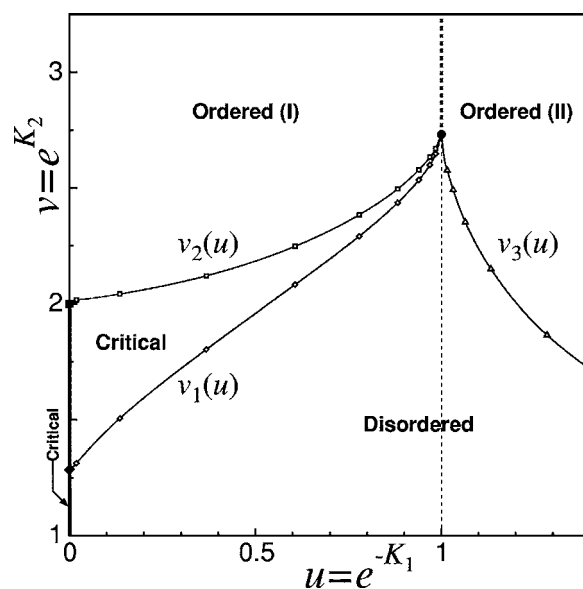


FIG. 2. The phase diagram of the model (1). The open diamonds (squares) with a curve exhibit the BKT line  $v_1(u)$  [ $v_2(u)$ ]. The filled diamond and the square on the  $v$  axis correspond to  $(0, v_1)$  and  $(0, v_2)$ , respectively. The filled circle at  $(1, 1 + \sqrt{3})$  denotes the decoupling point with  $\mathbf{Z}_3 \times \mathbf{Z}_3$  criticality. The open triangles with a curve exhibit the second-order transition line  $v_3(u)$ . The thick dotted line shows the first-order phase transition boundary.

Before moving to discussion, we shall check the consistencies among excitation levels on the BKT points. Since the amplitudes of logarithmic corrections are given by the operator-product-expansion coefficients, some universal relations among the scaling dimensions have been discovered [14,26]: For instance,  $[2\bar{x}_0(l) + \bar{x}_1(l)]/3 \approx 2$  at  $v_1(u)$  and  $[3x_2(l) + x_3(l)]/4 \approx \frac{1}{2}$  at  $v_2(u)$ . Here  $x_3(l)$  is the dimension of  $O_3 = \sqrt{2} \cos 3\sqrt{2}\phi$  [the bosonized expression of the staggered polarization  $P_j = (-1)^j \sum_{[j,k]} \delta_{\sigma_j, \sigma_k}$ ] which is  $\mathbf{S}_3$  invariant and odd for the sublattice symmetry [5,27]. In Table II, we give the scaling dimensions at  $K_1=1$ . Although  $\bar{x}_0(l)$  and  $\bar{x}_1(l)$  [ $x_2(l)$  and  $x_3(l)$ ] considerably deviate from the value for the free-boson case  $2$  ( $\frac{1}{2}$ ) due to the logarithmic corrections, their main parts cancel each other, so the average  $\bar{x}_{av} = (2\bar{x}_0 + \bar{x}_1)/3$  [ $x_{av} = (3x_2 + x_3)/4$ ] takes a value close to  $2$  ( $\frac{1}{2}$ ). The consistency checks can be satisfied only if the systems are on the BKT lines, and the investigated levels based on symmetry properties have the expected physical interpretations. Therefore, Table II is helpful to demonstrate the reliability of our phase diagram.

TABLE II. Examples of the  $L$  dependences of the scaling dimensions  $\bar{x}_0$  and  $x_2$  and the averages  $\bar{x}_{av}$  and  $x_{av}$  (see text) on the BKT points  $v_{1,2}(u)$  ( $K_1=1$ ). We extrapolate the finite-size estimates to  $L \rightarrow \infty$  using the least-squares fitting of the polynomial in  $1/L^2$ .

$L$	8	10	12	14	16	$\infty$
$\bar{x}_0(l)$	1.48366	1.52857	1.56357	1.59141	1.61404	
$\bar{x}_{av}(l)$	1.78633	1.83948	1.87883	1.90716	1.92759	2.006
$x_2(l)$	0.38137	0.38913	0.39454	0.39851	0.40155	
$x_{av}(l)$	0.50271	0.50078	0.49933	0.49811	0.49704	0.492

Finally, we discuss the nature of the phase diagram. As the real-space RG calculations predicted [12,25], the decoupling point  $(1, 1 + \sqrt{3})$  with  $\mathbf{Z}_3 \times \mathbf{Z}_3$  criticality (i.e.,  $c = \frac{8}{5}$ ) becomes unstable against relevant competing perturbations and exhibits crossovers to the behaviors controlled by the critical fixed points with lower symmetries [28]. One of those perturbations is the energy operator with scaling dimension  $\frac{4}{5}$ . For the ferromagnetic case  $u > 1$ , another one may be a product of order parameters on each sublattice which has the dimension  $\frac{4}{15}$ . Therefore, the crossover exponent  $\phi_F = (2 - \frac{4}{15}) / (2 - \frac{4}{5}) = \frac{13}{9}$  can predict the shape of the boundary around the point, and  $v_3(u)$  agrees with this [3]. Further, we obtain, for instance,  $c \approx 0.800$  at  $v_3(u)$  ( $K_1 = -0.25$ ), so the boundary can be regarded as a massless RG flow to the F3SP fixed point with  $c = \frac{4}{5}$ . On the other hand, we also analyze  $v_{1,2}(u)$ , and similar power law behaviors can be recognized. Although the estimated exponents take close values to  $\frac{13}{9}$ , the linearities of the log-log plots are rather lower than in the case of  $v_3(u)$ , and thus the estimates may acquire errors up to 10%. This may be due to the existence of the marginal operator in the intermediate critical region, which is absent in

the ferromagnetic case. Since the central charge takes the values, e.g.,  $c \approx 1.007$  and  $1.009$  at  $v_1(u)$  and  $v_2(u)$  ( $K_1 = 1$ ), respectively, the critical region can also be seen as a realization of the crossover to the Gaussian fixed point with  $c = 1$  [26,29]. However, its precise numerical analysis is still difficult, so this issue will be left as a future problem.

In summary, we investigated the square-lattice three-state Potts model with the ferromagnetic next-nearest-neighbor coupling. The phase diagram obtained here reveals features that could not be found in previous research. With the use of the level-spectroscopy method, we can break further ground for studying 2D classical systems with complex interactions. For more detailed study, we are now performing the Monte Carlo simulations, and we obtain preliminary data consistent with the present result of the phase diagram; they will be given in a forthcoming article.

One of the authors (H.O.) thanks M. Nakamura for stimulating discussions. This work was supported by Grants-in-Aid from the Ministry of Education, Culture, Sports, Science and Technology of Japan.

- 
- [1] E. H. Lieb, Phys. Rev. **162**, 162 (1967); E. H. Lieb, Phys. Rev. Lett. **18**, 692 (1967).
- [2] R. J. Baxter, J. Math. Phys. **11**, 3116 (1970); R. J. Baxter, Proc. R. Soc. London, Ser. A **383**, 43 (1982).
- [3] M. P. M. den Nijs, M. P. Nightingale, and M. Schick, Phys. Rev. B **26**, 2490 (1982).
- [4] J. K. Burton, Jr., and C. L. Henley, J. Phys. A **30**, 8385 (1997).
- [5] G. Delfino, J. Phys. A **34**, L311 (2001).
- [6] J. Kolafa, J. Phys. A **17**, L777 (1984); J.-S. Wang, R. H. Swendsen, and R. Kotecký, Phys. Rev. Lett. **63**, 109 (1989).
- [7] J. L. Cardy, J. L. Jacobsen, and A. Sokal, J. Stat. Phys. **105**, 25 (2001), and the references therein.
- [8] G. Delfino, in *Proceedings of the NATO Advanced Research Workshop on Statistical Field Theories*, edited by A. Cappelli *et al.* (Kluwer, Dordrecht, 2002).
- [9] H. Otsuka and Y. Okabe, Phys. Rev. Lett. **93**, 120601 (2004).
- [10] J. L. Cardy, Phys. Rev. B **24**, 5128 (1981).
- [11] G. S. Grest and J. R. Banavar, Phys. Rev. Lett. **46**, 1458 (1981); I. Ono, J. Phys. Soc. Jpn. **53**, 4102 (1984).
- [12] P. M. Oliveira, C. Tsallis, and G. Schwachheim Phys. Rev. B **29**, 2755 (1984).
- [13] J. C. Bonner and G. Müller, Phys. Rev. B **29**, 5216 (1984); J. Sólyom and T. A. L. Ziman, *ibid.* **30**, 3980 (1984); H. Inoue and K. Nomura, Phys. Lett. A **262**, 96 (1999).
- [14] K. Nomura, J. Phys. A **28**, 5451 (1995).
- [15] M. P. Nightingale and M. Schick, J. Phys. A **15**, L39 (1982); C. Jayaprakash and J. Tobochnik, Phys. Rev. B **25**, 4890 (1982).
- [16] E. H. Lieb, Phys. Rev. Lett. **18**, 1046 (1967).
- [17] R. J. Baxter, Ann. Phys. (N.Y.) **70**, 193 (1972).
- [18] H. Park, Phys. Rev. B **49**, 12881 (1994).
- [19] J. V. José, L. P. Kadanoff, S. Kirkpatrick, and D. R. Nelson, Phys. Rev. B **16**, 1217 (1977).
- [20] For the possibility of more efficient evaluation, see K. Nomura and A. Kitazawa, J. Phys. A **32**, 7341 (1998); H. Matsuo and K. Nomura (unpublished).
- [21] J. L. Cardy, J. Phys. A **17**, L385 (1984).
- [22] H. W. J. Blöte, J. L. Cardy, and M. P. Nightingale, Phys. Rev. Lett. **56**, 742 (1986); I. Affleck, *ibid.* **56**, 746 (1986).
- [23] J. L. Cardy, Nucl. Phys. B: Field Theory Stat. Syst. **270** [FS16], 186 (1986).
- [24] R. B. Potts, Proc. Cambridge Philos. Soc. **48**, 106 (1952); F. Y. Wu, Rev. Mod. Phys. **54**, 235 (1982).
- [25] J. M. J. van Leeuwen, Phys. Rev. Lett. **34**, 1056 (1975).
- [26] T. Ziman and H. J. Schulz, Phys. Rev. Lett. **59**, 140 (1987).
- [27] By denoting the interpenetrating sublattices of  $\Lambda$  as  $\Lambda_{\pm}$ ,  $(-1)^j$  is defined to take +1 for  $j \in \Lambda_+$  and -1 for  $j \in \Lambda_-$ .
- [28] A. B. Zamolodchikov, Pis'ma Zh. Eksp. Teor. Fiz. **43**, 565 (1986) [JETP Lett. **43**, 730 (1986)].
- [29] A crossover from  $c = \frac{3}{2}$  to 1 was discussed by A. Kitazawa and K. Nomura, Phys. Rev. B **59**, 11358 (1999).